MACHETTE AND PERSONIUS--MAP OF QUATERNARY AND PLIOCENE FAULTS IN THE EASTERN PART OF THE AZTEC 1° X 2° QUADRANGLE AND THE WESTERN PART OF THE RATON 1° X 2° QUADRANGLE, NORTHERN NEW MEXICO

SCALE 1:250,000

MAP MF-1465-B
(INCLUDES PAMPHLET)

AREA OF MAP

DEPARTMENT OF THE INTERIOR
U.S. GEOLOGICAL SURVEY

MISCELLANEOUS FIELD STUDIES
MAP MF-1465-B
PAMPHLET

MAP OF QUATERNARY AND PLIOCENE FAULTS IN THE EASTERN PART OF THE AZTEC 1° x 2° QUADRANGLE AND THE WESTERN PART OF THE RATON 1° x 2° QUADRANGLE, NORTHERN NEW MEXICO

By

Michael N. Machette and Stephen F. Personius

1984

INTRODUCTION

This map is the second of a series being compiled at a scale of 1:250,000 for the Rio Grande rift in New Mexico, western Texas, and southeastern Arizona (see index map). It shows known and inferred faults in the Taos Plateau and adjacent regions along which movement has taken place during the Quaternary or the Pliocene. The Taos Plateau, as defined by Upson (1939), occupies the eastern part of the Aztec 1° x 2° quadrangle and the western part of the Raton 1° x 2° quadrangle, northern New Mexico.

Although previous small-scale maps of the Rio Grande rift (Woodward and others, 1975; Hawley, 1978; Baldridge and others, 1983) show many of the features depicted in this map series, this series of maps is the first to focus specifically on faults and folds of less than 5 Ma. Preliminary analysis of the trend of faults throughout the Rio Grande rift (Machette and Colman, 1983) reveals a strong north-south orientation, whereas Miocene normal faults and dikes of the rift commonly have a northwest orientation (see least-principal-stress orientations of Zoback and Zoback, 1980; Zoback and others, 1981; Aldrich and Laughlin, 1982; and Lipman, 1983). This contrast in orientation indicates that the least principal stress may have rotated clockwise as much as 30° since 30 Ma (Machette and Colman, 1983).

Data used to compile this map come from published and unpublished geologic maps and literature, reconnaissance inspection of aerial photographs, and limited field investigations of Quaternary fault scarps. Sources of geologic data are quite variable, ranging from reconnaissance maps at scales of 1:62,500 or smaller to detailed maps at scales of 1:24,000 or larger. Where several sources of data were available, we used the most recent data from studies of late Cenozoic structure and stratigraphy.

This map shows data for some of the prominent faults in the map area, including amount of vertical surface offset (fault throw), age of faulted deposits, recency of fault movement (table 2 on accompanying map), and data on the morphology of fault scarps (table 3 in this pamphlet). Amounts of offset were determined in two ways: (1) from direct field measurements of the net vertical offset of surfaces across the fault, and (2) from interpretation of 1:24,000-scale topographic maps, photogrammetric analysis of aerial photographs, and from published data. The direct measurements are probably accurate to within 10 percent of the actual surface offset, whereas the second type of data usually reflects the range of values that are common along a fault, for example 5-20 m of surface offset.

Only faults that displace, or are suspected to displace, Pliocene or younger materials are shown on this map. Many more young faults may be present than are shown here. For example, Pliocene or younger faulting probably occurred but cannot be demonstrated in many areas of Miocene or older deposits; most faults in these areas are not shown. In other areas, deposition or erosion may have concealed or removed evidence of Pliocene and Quaternary faulting. Also, in areas of eroded basin-fill sediment many young faults lack clear surface expression; hence, because there is no cover of surficial material, finding evidence for faulting requires detailed geologic mapping of the basin fill and, unfortunately, maps of such areas are few.

Our approach of showing only faults for which direct evidence of Pliocene or younger movement exists produces a map showing a conservative number of faults and focuses the reader's attention on those faults that have demonstrable movement. Readers using this map for hazards assessment, regional structural analysis, or similar studies should be aware that many other young faults could be, and probably are, present within Miocene or older bedrock in the map area.

GEOLOGIC SETTING

Because the main subject of this report is faults that displace Pliocene and Quaternary deposits in the map area, we deal with the pre-Pliocene geology of the region only to the extent of presenting the basic structural setting of the Taos Plateau region of the northern Rio Grande rift. Recent reports on this area include discussions of the general evolution of the Rio Grande rift by Chapin (1979) and of the central Rio Grande rift by Baldridge and others (1980); a guidebook of the Rio Grande rift compiled by Hawley (1978); a description of upper Cenozoic sedimentary and volcanic rocks of the Taos area by Lambert (1966); the geology of the Taos Plateau by Lipman and Mehnert

(1979); the geology of the Española basin by Manley (1978, 1979); and a discussion of the structure and history of the Embudo fault-Jemez lineament by Muehlberger (1979). The following discussion presents a broad overview of the Rio Grande rift in northern New Mexico, the timing of the rift's inception, and its subsequent development during the late Cenozoic.

The area covered in this report includes the northern part of the Española basin, the Chama basin, and the Taos Plateau (the southern part of the San Luis basin as defined by Upson, 1939). These basins are separated by two major structural elements: (1) the Brazos uplift, a southeast-trending ridge of Precambrian basement rock (Cordell, 1978) that ends near Cerro Azul, and (2) the northeast-trending Embudo fault that parallels the Rio Grande in the southern part of the map area (Muehlberger, 1979). The Embudo fault is largely coincident with the Jemez lineament (Lambert, 1966; Cordell, 1978) where the lineament traverses the Rio Grande rift. Outside of the rift the lineament is marked by a northeast-trending alinement of Pliocene, Pleistocene, and Holocene volcanic centers (including the Jemez caldera) that extends from western New Mexico to southeastern Colorado (Lambert, 1966).

Rifting began between 32 Ma in southern New Mexico and as late as 27 Ma in northern New Mexico as regional extension reactivated Paleozoic and Mesozoic zones of weakness (mainly faults and folds) along the Southern Rocky Mountains. By 26 Ma, broad, shallow, fault-bounded basins had formed in central and southern New Mexico; these basins were filled by mafic flows, rhyolitic ash-flow tuffs, and locally derived volcaniclastic alluvium. Data from the Taos Plateau region suggest that here the rift had started to extend by 26-28 Ma (Chapin and Seager, 1975; Lipman and Mehnert, 1975); however, a period of pronounced extension had occurred in the Questa-Latir region, east of the Taos Plateau, by no later than 23 Ma (Lipman, 1981).

Chapin (1979) hypothesizes that as the rift opened, it broke en echelon across a series of structural flaws trending northeast and west-northwest that appear as lineaments in the basement terrane of the Southern Rocky Mountains. In the Taos Plateau region, basins formed on opposite sides of the Jemez lineament and developed opposing symmetries: hinged on the west (the San Luis basin) versus hinged on the east (the Española basin). The lineament forms a transition zone that marks a change in regional dip in adjacent rift basins; intrarift sediments are tilted to the west in the Española basin, and to the east in the San Luis basin. Stress along the Jemez lineament seems to have been relieved mainly by a scissor-like combination of normal and reverse faulting (Chapin, 1979; Muehlburger, 1979) rather than by strike-slip faulting as proposed by Kelley (1977).

The general Cenozoic structural pattern of the Taos Plateau region is that of a half graben having major displacement on the eastern margin of the rift, which here is coincident with the west front of the Sangre de Cristo Mountains. Gravity data suggest that this part of the rift is underlain by 5 km or more of basin-filling rocks (L. E. Cordell, unpub. data, 1979). Taking the amount of relief of the Sangre de Cristo Mountains into account, Precambrian to lower Tertiary rocks could be offset as much as 7-8 km along the east margin of the rift (Lipman and Mehnert, 1979). Conversely, the western margin of the rift is indistinctly marked by Servilleta Basalt that laps on eastward-tilted, pre-rift to early rift volcanic and sedimentary rocks. A zone of north- to northwest-trending, down-to-the-west antithetic normal faults that show small displacement and that cut upper(?) Miocene to lower(?) Pliocene Servilleta Basalt may be a faulted part of the western boundary of the Rio Grande rift.

Gravity data of Cordell (1978 and unpub. data, 1979) suggest several large displacement horsts and grabens beneath the cover of sedimentary and volcanic rocks along the axis of the Rio Grande rift in northern New Mexico. Oligocene volcanic rocks are exposed on a major north-trending horst beneath the central Taos Plateau in isolated hills south of Cerro Montoso and southeast of Cerro de la Olla, and in the San Luis Hills along the Colorado-New Mexico state line (Lipman and Mehnert, 1979). The northeast-trending Velarde graben (Manley, 1978; Golombek, 1983) in the northern part of the Española basin is bounded on the east by the Velarde fault (Manley, 1978) and on the west by the Pajarito fault (the Velarde and Pajarito faults are exposed mainly in the Albuquerque $1^{\circ} \times 2^{\circ}$ quadrangle). Although Manley (1978, p. 79) considered the Velarde fault as an extension of the previously unnamed Embudo fault, it may instead be a south-trending splay from the Embudo. If so, the Embudo fault may continue southwest as a down-to-the-south fault and join the Parajito west of the Rio Chama. Gravity data of Cordell (1978) and Budding (1978) suggest that the Velarde graben contains as much as 2.1-2.3 km of basin-fill sediment and thus forms the deepest part of the Española basin.

The central part of the map area is dominated by the Taos Plateau volcanic field (Upson, 1939; Lambert, 1966; Lipman and Mehnert, 1979). Tholeiitic flood basalt (Servilleta Basalt of Lipman and Mehnert, 1979; Baldridge and others, 1980), erupted exclusively from central shield volcanoes, is the most voluminous and widespread volcanic rock of the plateau. About 150 m of Servilleta Basalt is exposed in the Rio Grande gorge (central Taos Plateau), where as many as 15 flows form three sequences interbedded with sediment of the upper part of the Santa Fe Group (Lipman and Mehnert, 1979). Potassium-argon age determinations from Servilleta Basalt in the map area range from 2.8 to 4.6 Ma (table 1 on accompanying map), and Servilleta Basalt may be older as determined from stratigraphic position by Baldridge and others (1980). Although most of the basalt has been considered to be between 3 and 4 Ma (Lipman and Mehnert, 1979), Baldridge and others (1980) consider the Servilleta Basalt to be both late Miocene and early Pliocene.

The thick sequence of sedimentary rock of the Santa Fe Group preserved in the northern Rio Grande rift provides a stratigraphic record of the late Miocene to the Pleistocene(?). The Tesuque and Chamita Formations of the lower part of the Santa Fe Group (Galusha and Blick, 1971; Manley, 1978) and other coeval units to the south in the rift were deposited in a series of closed, fault-bounded basins; these rocks record the depositional response to Miocene rifting.

Renewed extension coupled with regional uplift and a subsequent increase in runoff in the early Pliocene (Chapin, 1979) resulted in the establishment of the Rio Grande as a major integrated system that flowed generally south through southern Colorado and New Mexico to northern Mexico. As the Rio Grande and its tributary streams traversed a series of elongate depressions (Hawley and others, 1976), they deposited a thick sequence of Pliocene and Pleistocene fluvial, bolson, and deltaic sediments that forms the upper part of the Santa Fe Group (the Ancha and Puye Formations here; the Sierra Ladrones Formation and Camp Rice Formation of Strain, 1966, to the south). Tilting during, or prior to, the early Pliocene created a strong unconformity that now separates the lower part of the Santa Fe Group from the overlying upper part of the Santa Fe Group. In the Española basin, the upper part of the Santa Fe Group is composed of fanglomerates derived from opposite sides of the rift; the Puye Formation was shed from volcanic highlands in the Jemez Mountains along the west side of the rift, and the Ancha Formation was shed from the Precambrian-cored Sangre de Cristo Mountains east of the rift (Manley, 1978). Main-stem alluvium deposited by the ancestral Rio Grande in Pliocene time is also included in the upper part of the Santa Fe Group.

Along the upper reaches of the ancestral Rio Grande (those parts in New Mexico and Colorado), deposition in the rift basins continued from 4-5 Ma to about 0.5 Ma, when the upper and lower reaches of the Rio Grande were connected at El Paso, Tex. Base level along the upper Rio Grande dropped drastically as a result of this integration; in response, the Rio Grande and its tributaries have cut deeply into basin-fill sediments throughout the rift, and in some places into the underlying bedrock.

METHODS FOR DETERMINING AGES OF FAULTING

Two methods are used in this study to determine the ages of fault movement. The first method is a stratigraphic approach by which the ages of the youngest faulted and oldest unfaulted deposits bracket the age of the most recent fault movement. Recurring episodes of movement are often recognized by comparing the cumulative amounts of displacement in deposits of various ages. A second method is an approach in which ages of undated fault scarps are based on a quantitative comparison of their morphology with morphologies of dated scarps. This latter approach is discussed in the section entitled "Fault-scarp morphology."

STRATIGRAPHIC METHODS

The distribution of young basin-fill deposits and volcanic rocks, surficial deposits, and some of the faults in the map area is taken from maps by Miller and others (1963), Lambert (1966), Kelley (1977), Manley and others (1978), and Lipman and Mehnert (1979). Their mapping was supplemented by reconnaissance of aerial photographs. Surficial deposits and young basin-fill deposits are here divided into four age categories to provide age control for recency of fault movement. The oldest deposits, of Pliocene and early Pleistocene age (5.0-0.75 Ma), include the Servilleta Basalt, local rhyolites to rhyodacites, and sediment between the volcanic rocks. This age category also includes upper Pliocene to lower(?) Pleistocene alluvial-fan and piedmont-slope basin-fill deposits immediately overlying the upper part of the Servilleta Basalt. The next category, middle and upper Pleistocene surfical deposits (750-150 ka and 150-10 ka, respectively), includes terrace, piedmont-slope, and alluvial-fan deposits that are graded to stream valleys incised into volcanic rocks of the Taos Plateau and into Miocene and older rocks of the Chama basin, west of the Taos Plateau. The youngest category is Holocene surficial deposits (less than 10 ka) that include alluvium of the lowest terraces and modern flood plains, young alluvial fans, and a thin blanket of eolian sand on the southern Taos Plateau.

Because detailed maps showing surficial geology are not available for most of the area, ages of the faulted deposits shown on the map were estimated on the basis of preservation of landforms, degree and density of dissection, stratigraphic and topographic position, and soil development. Although our geologic investigations were mainly of a reconnaissance nature, we feel confident that most of the age estimates for faulted and unfaulted deposits are reasonable because each category represents a broad range of geologic time.

FAULT-SCARP MORPHOLOGY

Studies by Wallace (1977) of slope degradation processes and the morphology of young fault scarps, and recent demonstration by Bucknam and Anderson (1979) of an empirical relation between the height of a fault scarp (H) and its maximum slope angle (θ) have established a basis by which the relative age of a fault scarp can be determined. We have used this empirical relation to estimate the recency of fault movement for some Quaternary faults in the map area.

The scarp-morphology data presented in the following discussion show the relation between fault-scarp height and maximum scarp-slope angle, the lateral variation of these two parameters, and their relation to fault scarps of known age. Our studies, as well as those of Bucknam and Anderson (1979), are based on the following premises of fault-scarp evolution: (1) the free face of the fault scarp is nearly vertical, in that it reflects the near-surface dip of the fault; (2) this face soon erodes by gravational collapse to the angle of repose of the faulted material, typically 32°-35°; and (3) from this point on, the slope of the scarp continues to decrease, but more slowly than before because slopewash is the dominant erosional process (Wallace, 1977; Nash, 1981). We have applied morphometric analysis only to those fault scarps formed in unconsolidated deposits, most of which are of Quaternary age. Most of the fault scarps studied are formed in pebbley sand to sandy gravel alluvium, materials that are generally of the same texture as the scarps studied by Bucknam and Anderson (1979).

Scarp nomenclature and measurement of scarp profiles

Heights of fault scarps were determined from detailed topographic surveys made along traverses perpendicular to the surface traces of faults in a manner similar to that described by Bucknam and Anderson (1979). We used a vernier-scale hand level and Jacobs staff, cloth tape, and stadia rod to measure slope angles across the scarp. The traverses extended 20-100 m above and below the fault scarp to determine the slopes of the adjacent alluvial surfaces. Measurements were made at intervals of 2-5 m on the upper and lower slopes and at intervals of 0.5-2 m on the scarp itself. Scarp profiles were drawn from these measurements using a computer-plotting routine supplied by R. C. Bucknam.

The nomenclature used in this report is modified only slightly from that suggested by Bucknam and Anderson (1979). Scarp height (H, in meters; fig. 1) is defined as the vertical separation between the intersections of the plane of maximum scarp-slope angle and the surfaces above and below the scarp. The angles θ and γ denote the inclination (with respect to horizontal) of the scarp and the adjacent land surfaces, respectively. For determining H in an ideal case, the surfaces flanking the scarp are parallel and horizontal or only gently sloping (γ less than 3°-5°). The maximum scarp-slope angle (θ) was measured over a length equal to 10-20 percent of the distance between the crest and toe of the scarp at four to six locations adjacent to each traverse line. The values of θ reported here are the averages of the repeated measurements. Thus, each traverse yielded a scarp profile and a measurement of H and θ (a data pair). To treat these data statistically, we required that the minimum data set from any one continuous portion of a scarp consist of at least seven data pairs. Data sets smaller than seven pairs may or may not be representative of the morphology of a fault scarp; however, these smaller data sets still are useful as general indicators of the height and steepness of a fault scarp.

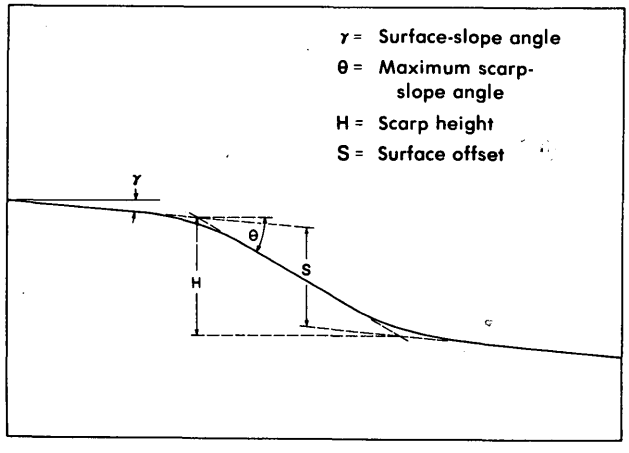

Figure 1.—Diagrammatic profile of a hypothetical fault scarp (modified from Bucknam and Anderson, 1979, fig. 1).

Along any one fault, we attempted to measure a variety of scarp heights; these generally ranged from about 1 to 10 m, although some scarps are as much as 30 m high. Scarp profile sites were chosen on the basis of relative surface stability; areas were avoided where recent erosion or deposition may have diminished or partly buried the fault scarp. Accumulations of eolian sand in many parts of the Rio Grande rift have buried fault scarps and thus made large tracts of ground unsuitable for studies of fault-scarp morphology. Where fault scarps are discontinuous, form en echelon patterns, or are segmented (segments are sections of faults each having a history of discrete surface rupture), we tried to collect several discrete data sets along individual parts of each fault. Unfortunately, the number of scarp profiles measured in this reconnaissance study is small because of limited field time, narrow range in scarp heights, and a lack of abundant, suitable sites.

Relation between maximum scarp-slope angle and scarp height

The studies of Bucknam and Anderson (1979) have shown that a statistically significant correlation exists between the height (H) and the maximum scarp-slope angle (θ) of scarps formed by a single rupture event (fig. 2). The relationship holds for a wide range of heights and slope angles on fault scarps and also for wave-cut shoreline scarps, such as those formed during the highest stand of Lake Bonneville in Utah. Using a least-squares linear-regression equation having the form $y = a + bx$ (where a is the y-axis intercept, b is the slope of the line, y is θ and x is H), they found that for the Lake Bonneville shoreline, 91 percent of the variation in the two parameters is explained by the equation, $\theta = 3.8 + 21.0(\log H)$ (R. C. Bucknam, written commun., 1980). They also found that scarps both younger and older than the Lake Bonneville shoreline have similar relations, but plot in respectively higher and lower parts of the graph of θ versus H. Their finding suggested to us that scarp morphology might be useful for differentiating the ages of Quaternary faulting over large areas of the Rio Grande rift.

The presentation of scarp-morphology data in this report follows the style of Bucknam and Anderson (1979); a hypothetical scarp profile is illustrated in figure 2. Data pairs are plotted as filled circles and, where there are at least seven data pairs, the equation for the line of best fit and the coefficient of determination (r^2) are included. We have noted two conditions for which the empirical relation between H and θ is not consistent. The first condition involves fault scarps having maximum scarp-slope angles (θ) that are only several degrees steeper than those surfaces adjacent to the scarp; such scarps generally have a weaker correlation between H and θ. The second condition involves scarps formed on land surfaces having originally steep gradients (γ), those of more than 5°-10°. In such cases, values of θ can only approach the bounding limit γ, and thus these scarps have inherently large values of θ and yield erroneously young inferred ages.

The methods and results of Bucknam and Anderson (1979) and Machette (1980 and data in Pierce, 1981) were used to assign relative ages to fault scarps from the morphometric data. The lines of best fit for two sets of data were used for comparison in figure 2 and on similar plots of scarp-morphology data (figs. 4-9). The uppermost dashed line (labelled 5K in fig. 2) represents combined data from two fault scarps in New Mexico: a fault near the Cox Ranch, just west of White Sands (most recent movement about 4 ka; data of L. H. Gile and M. N. Machette in Seager, 1981); and segment C of the La Jencia fault near Magdalena (most recent movement about 5 ka; Machette, 1980; data of Machette in Pierce, 1981). The second dashed line (labelled 15K in fig. 2) is based on R. C. Bucknam's data (written commun., 1980) from the highest wave-cut shoreline of Lake Bonneville, Utah, which is here considered to have formed about 15 ka on the basis of stratigraphic studies by Scott and others (1983). Although the Lake Bonneville shoreline escarpment is an erosional feature, Bucknam and Anderson (1979) consider that it is eroded much like a fault scarp. The main difference in these two genetically different features is that a fault scarp requires an initial time interval for the free face to collapse and for the scarp slope to decrease to the angle of repose, whereas a shoreline escarpment probably has an initial scarp-slope angle that is equal to, or slightly less than, the angle of repose (instead of nearly vertical). The time needed for the scarp to degrade in such a manner has not been determined, but the degree of erosion of historic scarps in the Basin and Range Province suggests to us that this interval is only several hundred years to perhaps a thousand years long.

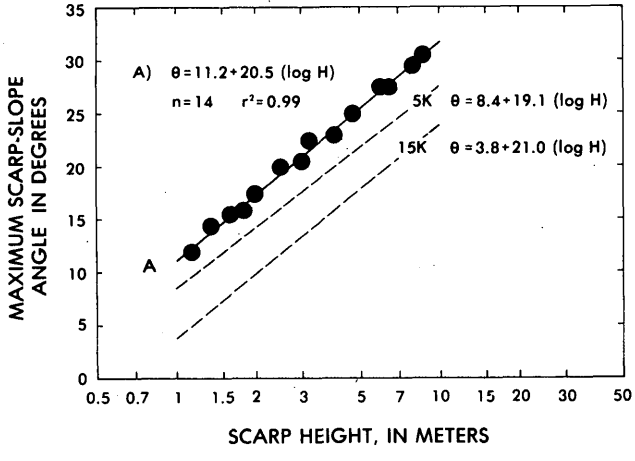

Figure 2.--Maximum scarp-slope angle (θ) plotted against scarp height (H) for a hypothetical fault scarp (line A). Also shown are the number of data pairs (n), the coefficient of determination (r^2), two reference lines for age comparisons, 5K (4-5 ka) and 15K (15 ka), and equations for their lines of best fit.

Major factors that affect the rate of scarp degradation include the texture and cohesion of the faulted deposits, orientation of the scarp, and the climate, vegetation, biologic activity, and topographic relief at the scarp site. We chose profiling sites where these characteristics were as uniform as possible, so that observed differences in scarp morphology would largely reflect the age of a scarp. However, variations do exist between some scarps, especially in the texture of the faulted deposits. Thus, so as not to overinterpret our morphometric data, we chose the following criteria to assign relative ages to fault scarps: (1) scarps having data sets that lie above the upper dashed line (5K) are considered to be of Holocene age (less than 10 ka); (2) those data sets that lie between the two dashed lines indicate scarps of Holocene or latest Pleistocene age (10-25 ka); and (3) those data sets that lie to the right of and below the lower dashed line (15K) indicate scarps of late Pleistocene age (10-150 ka) or, less likely, of middle Pleistocene age (150-750 ka).

COMPOUND FAULT SCARPS

Some fault scarps in the map area were formed by multiple episodes of surface rupture as evidenced either by decreasing scarp heights in progressively younger deposits (see above example) or by scarps that have discrete facets (that is, compound-slope angles), as recognized by Wallace (1977). These compound fault scarps represent degraded fault scarps that have been refaulted one or more times (the older scarp slopes are noted by the angle θ', fig. 3). We interpret many compound scarps by assuming that the steepest portion of the scarp (Hs, fig. 3) is formed by the most recent episode of faulting and that Hs is close enough to the amount of recent offset that a plot of Hs versus θ for a compound scarp (recurrent movement) and a plot of H versus θ for an adjacent single-event scarp will yield similar morphometric relations. Hs, the

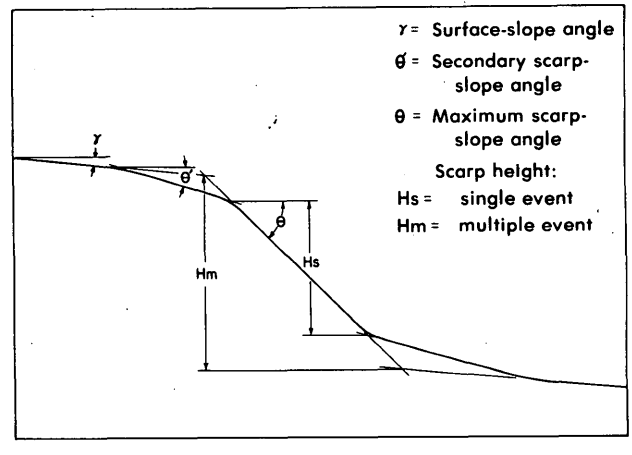

Figure 3.--Diagrammatic profile of a hypothetical compound fault scarp.

youngest element of the total scarp height (Hm, multiple event), is here defined as the difference in elevation between the intersections of the old scarp surfaces (θ') and the plane of the maximum scarp-slope angle (θ, fig. 3). Although values of Hs are only crude estimates of the heights of most recent scarps, measurements of Hs nonetheless are useful. When treated in such a manner, compound fault scarps yield values for Hs versus θ (open circles in fig. 4) that plot to the left of values for Hm versus θ (filled circles in fig. 4). Note that the resultant lines of best fit for Hs data commonly have steeper slopes (larger values for b in the regression equation) than Hm data and that these b values are similar to those noted in single-event scarps. Conversely, a fault scarp represented by a line of best fit having a low b value might indicate multiple episodes of faulting even though its resultant scarp may not have compound slope angles.

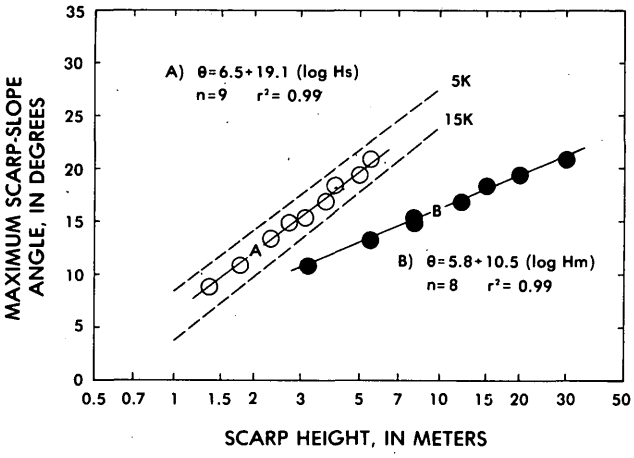

Figure 4.--Maximum scarp-slope angle (θ) plotted against scarp heights (Hs and Hm; lines A and B, respectively) for a hypothetical compound fault scarp. Also shown are the number of data pairs (n), the coefficient of determination (r^2), two reference lines for age comparisons, 5K (4-5 ka) and 15K (15 ka), and equations for lines of best fit A and B.

INTERPRETATIONS OF FAULT BEHAVIOR AND HISTORY

The following examples show how patterns of surface rupture, amounts of surface offset, and ages of faulted deposits can be used to decipher the movement history of a particular fault or fault zone.

SCARPS PRODUCED BY A SINGLE EPISODE OF MOVEMENT

Fault scarps produced by a surface rupture or a combination of ruptures closely spaced in time (here referred to as a single episode of faulting) typically have only a limited range of heights even though they are formed in deposits of different ages. The following example shows a fault as it could appear on the accompanying map, and, in fact, many young fault scarps in the Rio Grande rift have such histories of movement and patterns of offset.

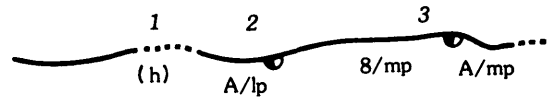

1. Deposits of Holocene age (h) are not offset.
2. Deposits of late Pleistocene age (lp) are offset less than 5 m (A).
3. Deposits of middle Pleistocene age (mp) are offset amounts less than 5 m (A) to as much as 8 m.

These data indicate that the most recent faulting occurred in the late Pleistocene because the fault displaces upper Pleistocene deposits, but does not displace Holocene deposits. Although the amount of offset varies somewhat along the length of the fault, the scarp is the product of a single episode of movement. Because the amounts of offset in deposits of both late and middle Pleistocene age are similar, this fault scarp probably was produced during only the late Pleistocene. This age is indicated by a half-filled semicircle shown on the the downdropped side of the fault.

SCARPS PRODUCED BY RECURRENT MOVEMENT ON A FAULT

Recurrent movement on faults is easily recognized because the resultant scarps in old deposits are higher than those in young deposits. The following example shows hypothetical data from a scarp produced by recurrent movement. Many of the faults that cut middle Pleistocene to Pliocene deposits in the Rio Grande rift show evidence of recurrent movement.

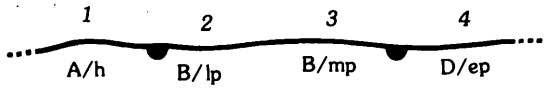

1. Deposits of Holocene age (h) are offset less than 5 m (A).
2. Deposits of late Pleistocene age (lp) are displaced 5-20 m (B).
3. Deposits of middle Pleistocene age (mp) also are offset 5-20 m.
4. Deposits of early Pleistocene to Pliocene age (ep) are offset 50-150 m (D).

This fault pattern indicates recurrent movement since at least the early Pleistocene because early Pleistocene to Pliocene deposits are offset greater amounts than those of middle Pleistocene age, and the Holocene deposits are offset least of all. The most recent faulting is Holocene, shown by a filled semicircle on the downthrown side of the fault. Additional evidence of recency of faulting might come from data on the scarp's morphology, such as that presented later in the report.

SCARPS PRODUCED BY MOVEMENT ON SEGMENTS OF A FAULT

Many fault scarps form along discrete lateral segments of a fault, as recognized by differing ages of the most recent faulting event along the length of a fault. These segments are commonly separated by unbroken ground, en echelon steps, or changes in the trend of a fault scarp. The following example shows a segmented fault that has nearly equal amounts of surface offset along its length, but markedly different ages of movement on separate segments as determined by fault-scarp morphology (see discussion of scarp morphology below) or other dating techniques. On cursory inspection, this fault appears to be the product of a single episode of movement (see first example).

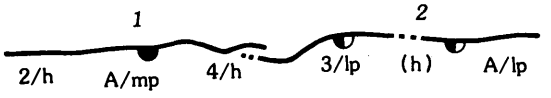

1. Along one segment of the fault, deposits of Holocene (h) age and middle Pleistocene (mp) age are offset similar amounts (2-4 m and less than 5 m, respectively).
2. Along another segment of the fault, late Pleistocene deposits (lp) are offset less than 5 m (A), whereas intervening Holocene deposits (h) are not displaced.

These data indicate that the most recent faulting was Holocene along the first segment of the fault, but was late Pleistocene (shown by half-filled semi-circle) along the second segment. Studies of fault-scarp morphology in the Rio Grande rift of New Mexico and western Texas (Machette, unpub. data, 1983) confirmed, for many faults, that segments moved at different times, so that the resultant scarps vary widely in both height and morphology along a single fault or fault zone.

PROMINENT QUATERNARY FAULTS

Most of the following information is based on field investigations conducted during the summers of 1980 and 1981, although some data were available from the published results of others. The faults are keyed by number to the map, and pertinent data for the faults are summarized in table 2 on the accompanying map and table 3 near the end of this pamphlet.

MESITA FAULT (1)

The Mesita fault, first mapped by Colton (1976), extends from about 5 km north of Mesita cone, in southern Colorado, to the east flank of Ute Mountain, in northern New Mexico. Only the southern 7 km of its 22-km trace extends into New Mexico. The Mesita fault (Kirkham and Rodgers, 1981, fault 108) forms a conspicuous west-facing scarp along the east side of the Sky Valley Ranch 7 1/2-minute quadrangle (Colorado) where it offsets the west flank of the Mesita cone (a Quaternary basalt eruptive center; Tweto, 1979) about 13 m down to the west (Kirkham and Rodgers, 1981, p. 25). A strong calcic soil has developed in a blanket of eolian sand and reworked basaltic cinders 2-3 m thick that overlies the basalt. Elsewhere on the Taos Plateau such soils are common in middle to lower(?) Pleistocene alluvium.

South of Mesita cone, the Mesita fault forms 5- to 7-m-high, south-trending scarps in lower(?) to middle Pleistocene piedmont-slope alluvium. In New Mexico, the fault forms smaller scarps, 2-5 m high, in middle to upper(?) Pleistocene alluvium. These latter scarps are discontinuous, moderately eroded, and dissected by streams; their gross morphology suggests the most recent faulting is late Pleistocene, but not latest Pleistocene.

According to Burroughs (1978), drilling in the area shows that the Servilleta Basalt is offset only 15-30 m by the Mesita fault. If so, then much of the fault's Pliocene and younger offset is recorded in the scarps on Quaternary Mesita cone, which is offset 13 m.

SUNSHINE VALLEY FAULTS (2)

Colton (1976) mapped a series of north-trending faults, here collectively named the Sunshine Valley faults, across Sunshine Valley, between Guadaloupe and Ute Mountains. The longest of these suspected faults extends north 22 km from a southern fork of Latir Creek to a point 6 km east of Ute Mountain. Although Colton regarded these faults as the southern extension of the Mesita fault (1), we consider them as separate features because they are not continuous with the Mesita fault and because they have the opposite sense of movement, down to the east.

The Sunshine Valley faults cross an area underlain by upper Pleistocene alluvium; however, 1-2 km west (downslope) of the main fault, middle(?) Pleistocene alluvium forms elongate ridges 5-10 m above stream level. Any or all of these ridges may be the result of uplift along the Sunshine Valley faults. The longest and easternmost of the Sunshine Valley faults is the only one that coincides with an obvious alinement of vegetation. We could not find a topographic escarpment along this lineament; however, the fine-grained sediment along the east side of this lineament probably was ponded on the downthrown, upslope side of a small fault scarp that is now largely buried. If the Sunshine Valley faults cut upper Pleistocene alluvium, their offsets must be small, less than 5 m. The three suspected faults that Colton (1976) mapped south of Sunshine and west of the main fault could not be found in the field.

SANGRE DE CRISTO FAULT ZONE (3, 4, 5, 6)

The Sangre de Cristo fault zone is one of the major Pliocene and Pleistocene structures in the map area. The fault zone bounds the west side of the Sangre de Cristo Mountains along most of their 160-km length in southern Colorado and northern New Mexico. Scott (1970) first mapped many of the faults in this zone, and recently Kirkham and Rodgers (1981) and McCalpin (1983) have demonstrated that Holocene or late Pleistocene movement occurred along most of the

zone in Colorado. However, information about the fault zone in New Mexico is limited to our sparse scarp-morphology data collected along faults in the Costilla area (Cedro Canyon fault, 3; Urraca Ranch fault, 4) and the Taos area (Taos Pueblo fault, 5; Cañon fault, 6).

The main fault of the Sangre de Cristo fault zone lies along the west side of San Pedro Mesa in southernmost Colorado and along the west side of the Sangre de Cristo Mountains in northernmost New Mexico. Kirkham and Rodgers (1981) refer to this as the West San Pedro Mesa fault. San Pedro Mesa is capped by Servilleta Basalt (3-4 Ma) that lies on poorly consolidated sediment of the Santa Fe Group, and, as a result, the fault is covered by landslide debris along most of its length. Burroughs (1978) estimates that the basalts west of the West San Pedro Mesa fault have been downdropped at least 600 m, corresponding to an average uplift rate of 150-200 m/m.y. during the Pliocene and Quaternary.

Immediately southeast of Costilla, the southernmost remnant of the basalt of San Pedro Mesa is uplifted 240-360 m above the adjacent plain of the Taos Plateau. This same basalt is not exposed immediately west of the fault, but must be present at depth; thus, the topographic separation between the uplifted basalt and the adjacent valley floor to the west represents the minimum amount of offset along this part of the fault zone in the past 3-4 Ma. Here the corresponding minimum average rate of uplift is 60-120 m/m.y.

The Sangre de Cristo fault zone is shown on the accompanying map as a dotted or dashed line along most of the range front from the state line south to the Taos area. We found prominent fault scarps only along a small portion of the range front; such a distribution indicates either that late Quaternary movement is limited to specific segments of the fault zone or that erosion and deposition have removed the fault scarps in many places. Both may be occurring. Nevertheless, it seems apparent from the morphologies of scarps and stratigraphic evidence discussed here that the Sangre de Cristo fault zone consists of a series of parallel to subparallel faults each of which have discrete segments that have individual displacement histories related to both the regional and local stress fields and to inherent structural boundaries that separate fault segments. In New Mexico, the Sangre de Cristo fault zone appears to have a history of less active late Quaternary displacement than it has to the north in Colorado, where pervasive Holocene and late Pleistocene deformation has been documented by Kirkham and Rodgers (1981) and by McCalpin (1983). However, the Sangre de Cristo fault zone shows a substantial amount of Pleistocene and Pliocene offset, at rates that are similar to other rift-bounding faults, such as those in the Socorro area of New Mexico (Machette and McGimsey, 1983).

Cedro Canyon fault (3)

The Cedro Canyon fault extends from a point 5 km south of Costilla, N. Mex., south and south-southwest about 7 km. This fault appears to be a westward splay of the main range-bounding fault, which is poorly expressed in this area. The fault is named here for Cedro Canyon, the source area for a series of alluvial-fan deposits that are partly cut by the fault. Upson (1939, p. 731), who first recognized this fault scarp, showed it in a northeast view (his fig. 6) as photographed from a point about 6.7 km south of Costilla on New Mexico State Highway 3. Here the fault forms a conspicuous, nearly continuous scarp 4-14 m high, 0.25-1 km east of the highway. Interestingly, recent maps of the area (McKinlay, 1956; Colton, 1976) do not show this prominent fault.

The Cedro Canyon fault offsets locally derived alluvial-fan debris of late to middle Pleistocene and possibly early Pleistocene age. However, the most recent sediments of the Cedro Canyon alluvial fan are probably latest Pleistocene to Holocene, and these sediments bury the fault scarp at its north end. Although Upson (1939) considered the fault to be Holocene, our stratigraphic evidence suggests that the most recent fault movement must predate deposition of latest Pleistocene fan alluvium; however, the scarp-morphology data suggests that it need not be much older.

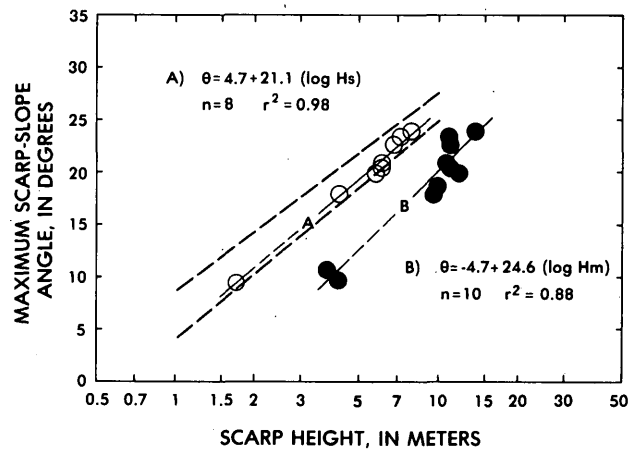

Figure 5.--Maximum scarp-slope angle (θ) plotted against scarp heights (Hs and Hm) for the Cedro Canyon fault (fault 3 on the accompanying map). Open circles (line A) are for most recent single-event part of scarp; filled circles (line B) are for entire multiple-event scarp.

Scarps along the Cedro Canyon fault record multiple episodes of surface rupturing. The largest scarp (more than 8-9 m high) is in old alluvium along the northern 2 km of the fault, and commonly has compound scarp-slope angles indicating young movement superposed on an old, degraded scarp (table 3). South of the road to Urraca Ranch (presently the Urraca Wildlife Refuge), a single-event scarp less than 4 m high is formed in young alluvium (upper Pleistocene?). Figure 5 shows the relation between both single-event (Hs) and multiple-event (Hm) scarp heights and maximum scarp-slope angles (θ) for the

Cedro Canyon fault. These data suggest that the most recent episode of movement was in the latest Pleistocene (10-25 ka) and produced scarps of less than 2 to about 8 m high (Hs values). At least two episodes of movement are recorded by scarps of the Cedro Canyon fault. The surface of the fault is nowhere exposed, but we suspect that it has a normal sense of displacement and probably dips steeply to the west.

Urraca Ranch fault (4)

Upson (1939, p. 731) pointed out a second fault in the Costilla area, here named the Urraca Ranch fault. This fault is along the mountain front and forms a prominent scarp across the head of an alluvial fan at the mouth of Jaroso Canyon (La Jara Creek in Upson, 1939). The scarp is preserved for only a short distance adjacent to Jaroso Canyon; it is eroded or poorly preserved both to the north and south along the mountain front. Although the Urraca Ranch fault is but a small part of the major range-bounding fault zone of the Sangre de Cristo Mountains, it shows that this fault zone has been recently active.

The soil in the fan alluvium is judged to have formed since either the early late Pleistocene or the late middle Pleistocene (several hundred thousands of years) on the basis of a reddish-brown, clay-enriched (argillic) B horizon 0.5-1 m thick present in the upper part of the alluvium. Upson (1939) reported the scarp to be about 70 ft (21 m) high, but the scarp we measured at Urraca Ranch is but 16.5 m high (Hm) and has a θ of 16°-17°. This scarp is more degraded than scarps of similar height along the Cedro Canyon fault (fig. 5) and lacks a discernible compound profile. However, its height alone suggests several episodes of movement since the middle Pleistocene, the most recent of which could have been during the late Pleistocene because the scarp still has a relatively large θ.

Taos Pueblo fault (5)

The Taos Pueblo fault forms a sinuous escarpment that trends roughly northwest and southwest, north and south of the Taos Pueblo, respectively. This fault is a part of the range-bounding fault zone along the west base of the Sangre de Cristo Mountains. The fault is separated into two segments by the Rio Pueblo de Taos as it emerges from the mountains. The height of scarps along the Taos Pueblo fault ranges from 2 to 18 m along the northern segment and from 2 to 7 m along the southern segment (table 3).

The northern segment of the fault typically has a scarp 8-15 m high that locally splits into two closely spaced scarps, each 5-12 m high. Due north of the Taos Pueblo, this fault cuts lower(?) to middle Pleistocene coarse-grained fan alluvium along a northwesterly trend. Farther to the north, the fault trends north, parallel to and west of the mountain front, where it displaces upper(?) Pleistocene alluvium less than 2 m. Scarp-morphology data from the northern segment (fig. 6) show clear evidence of recurrent fault movement, the most recent of which produced scarps 3-7 m high during the late Pleistocene.

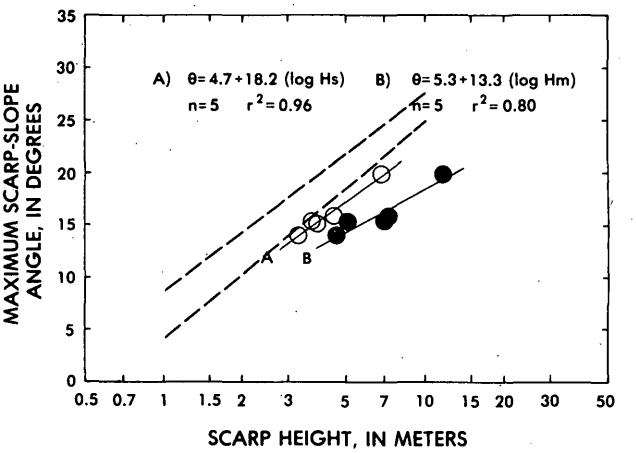

Figure 6.--Maximum scarp-slope angle (θ) plotted against scarp heights (Hs and Hm) for the northern segment of the Taos Pueblo fault (fault 5 on the accompanying map). Open circles (line A) are for most recent single-event part of scarp; filled circles (line B) are for entire multiple-event scarp.

The southern segment of the fault forms two nearly parallel southwest-trending scarps in middle to upper Pleistocene piedmont-slope alluvium. These scarps are generally less than 2-3 m high, but they join about 2 km south of the Pueblo to form a single scarp 5-7 m high. The most recent rupture on the combined fault produced scarps 3-4 m high (Hs, fig. 7) during the late Pleistocene, as indicated by the compound nature of the scarp. However, this most recent episode of movement may not be as young as that along the northern segment of the Taos Pueblo fault.

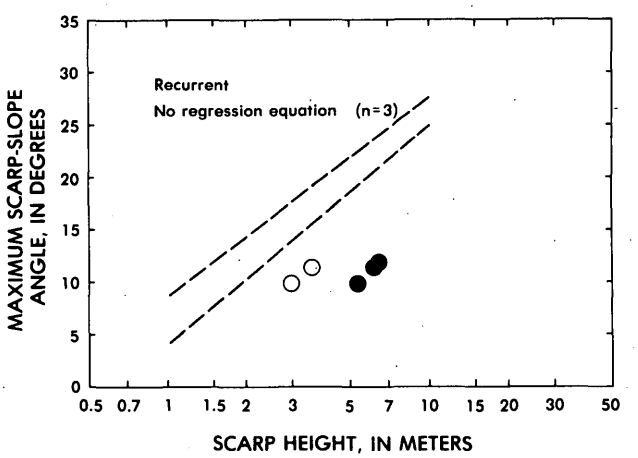

Figure 7.--Maximum scarp-slope angle (θ) plotted against scarp heights (Hs and Hm) for the southern segment of the Taos Pueblo fault (fault 5 on accompanying map). Open circles are for most recent single-event part of scarp; filled circles are for entire multiple-event scarp.

The two segments of the Taos Pueblo fault form single, double, and compound scarps of late Pleistocene age along a curving, concave-westward trace about 10 km long. Both segments of the fault are 0.5-1.5 km basinward of the mountain front and displace Pleistocene alluvium. The fault probably dips steeply to the west and has normal dip-slip movement.

Cañon fault (6)

The Cañon fault forms small scarps east and south of Cañon, a small town 1.6 km east-southeast of Taos, N. Mex. (Cañon is not shown on the base for the accompanying map). These scarps are the southernmost surface expression of the Sangre de Cristo fault zone and join the west end of the Embudo fault (8) that strikes northeast from Hondo Canyon along the base of the Picuris Mountains (Muehlberger, 1979). We traced the Cañon fault scarps from the north side of Rio Fernando de Taos (due east of Cañon), where the fault places Pleistocene alluvium in contact with Pennsylvanian rocks on the east (Lambert, 1966), south and southwest to 1.5 km north of Talpa, a distance of about 6 km. South of the Rio Fernando de Taos, the fault cuts upper and middle to lower(?) Pleistocene piedmont-slope alluvium. The scarp-morphology data (fig. 8, table 3) show multiple-event heights (Hm) of 3.5-5.4 m and single-event heights (Hs) of 1.8-3.4 m. The most recent of recurrent movements on the Cañon fault was during either early(?) Holocene or latest Pleistocene.

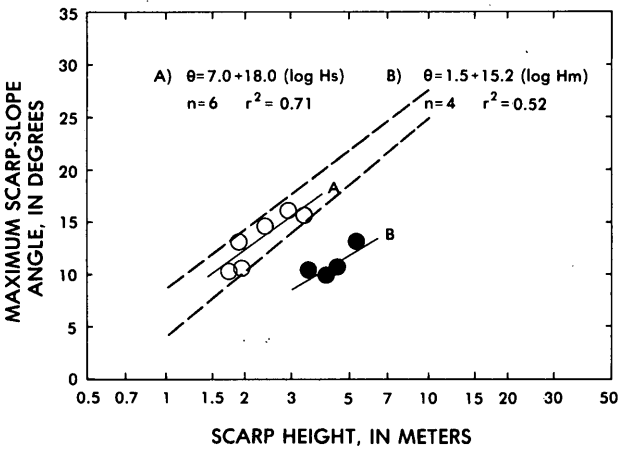

Figure 8.--Maximum scarp-slope angle (θ) plotted against scarp height (Hs and Hm) for the Cañon fault (fault 6 on the accompanying map). Open circles (line A) are for most recent single-event part of scarp; filled circles (line B) are for entire multiple-event scarp.

LOS CORDOVAS FAULTS (7)

Los Cordovas faults are here named to designate a zone, 5-8 km wide, of north-trending normal faults that extend about 12 km northward from the Rio Taos, near Los Cordovas, N. Mex., to just south of U.S. Highway 64, which crosses the Rio Grande gorge west of Taos. In areas of greatest offset, the faults place gravelly piedmont-slope alluvium (Lambert, 1966) down to the west against stratigraphically lower Servilleta Basalt (Lambert, 1966, p. 47). The alluvium is probably no older than late Pliocene or early Pleistocene, but clearly is older than the sequence of alluvium that forms terraces associated with major streams in the Taos area. By this reasoning, movement on Los Cordovas faults may be as old as early Pleistocene, but could be considerably younger (middle? Pleistocene).

Erosion of the piedmont gravel has produced west-facing scarps 15-30 m high. However, the fault offset is undoubtedly more. Most of the faults are poorly exposed because they are covered by alluvium that fills structurally controlled south-trending valleys. However, Lambert (1966, p. 47) reports that one of the faults dips 89° to the west where it is exposed 2 km southwest of Los Cordovas.

Lambert (1966, his fig.1) shows only the more prominent of Los Cordovas faults. Our photo reconnaissance confirms that most of the drainage pattern between the Rio Taos and the axis of the arch (anticline), as mapped by Muehlberger (1979, fig. 2), is structurally controlled by north-trending Los Cordovas faults. Because the faults do not continue much north of the axis of the arch, the streams here flow west, down the piedmont slope toward the Rio Grande. Near Los Cordovas, the Rio Taos follows a nearly straight course parallel to the axis of the Gorge arch, and that course suggests to us that the river occupies the axis of a previously unmapped syncline. Muehlberger and others (1983) suggested that the Gorge arch (and by association the inferred syncline) resulted from northwestward-directed compression and thrusting of the Picuris Mountains block over the southern Taos Plateau along the Embudo fault (8) during the late Cenozoic.

EMBUDO FAULT (8)

The Embudo fault extends 75 km along a general trend of N. 60° E. and bounds the northern part of the Española basin and the southern part of the San Luis basin. According to Muehlberger (1979, p. 81), the Embudo is both a hinge zone and a transform fault (a sinistral, oblique-slip reverse fault) that obliquely spans the Rio Grande rift. The few exposures of the northeastern part of the Embudo fault have high to low dips and reverse movement, whereas the inferred movement along its southeastern part is normal (of unknown dip). The fault changes from normal to reverse sense of movement through a hinge point near Embudo, where both northward and southward downdip movement is recorded in the Servilleta Basalt. The southern end of the Embudo fault is here considered to be the north margin of the Española basin.

Kelley (1977, p. 54) proposed that extension of the Rio Grande rift has not been perpendicular to the rift's axis (generally north to south), but rather has been slightly oblique, which has resulted in a sinistral component of movement parallel to the rift. Reverse movement along the northeastern part of the Embudo

fault supports this hypothesis, for if extension is strictly perpendicular to the rift's length, the Embudo would show oblique-normal movement owing to its orientation of N. 60° E. (Muehlberger, 1979). However, oblique-slip movement has not been proven by previous workers. Muehlberger proposed (1979, p. 80) that the fault may offset Precambrian rocks as much as 3,000 m between the uplifted Picuris Mountains south of the Embudo fault and the deepest part of the basin north of the fault.

Muehlberger's detailed maps (1979) of road cuts near Hondo Canyon show convincingly that the Embudo fault has reverse movement. In the northernmost roadcut (Muehlberger, 1979; roadcut 1, his fig.4), very coarse grained Pliocene alluvium of the Servilleta Formation (his terminology) is thrust over finer grained lower(?) to middle Pleistocene post-Servilleta alluvium and fault-scarp colluvium. Our Pleistocene age for the tectonically buried sediment is based on the presence of a well-developed calcic soil having a discontinuous stage-III to stage-IV K horizon.

We measured two scarp profiles on the piedmont slope adjacent to and above Muehlberger's roadcut 1 (1979, his fig. 3). Northeast of the road cut, the scarp is about 15 m high, whereas to the southwest it is only 7 m high (fig. 9, table 3). However, the crest and backslope of the smaller scarp has been eroded, and its height is therefore a minimum value. The morphology of the fault scarp is similar to scarps formed by late Pleistocene normal faults, although we cannot be certain that such comparisons are valid.

Northeast of Hondo Canyon, the Embudo fault splits into several parallel splays that form low, discontinuous scarps in lower to middle(?) Pleistocene sediments. This part of the fault is inferred to continue eastward along the base of the Picuris Mountains and to structurally connect with the Cañon fault, southeast of Ranchos de Taos.

CONCLUSIONS

Quaternary and Pliocene faults are abundant in the Taos Plateau region of the Rio Grande rift in northern New Mexico. In the map area, faults cut lower(?) Pleistocene to uppermost Pleistocene sediment, upper Miocene to Pliocene basalts, and Pliocene to lower(?) Pleistocene basin-fill deposits. Morphologic, pedologic, and geologic data collected along some of the major Quaternary fault scarps indicate that many were formed during the late Pleistocene (150-10 ka), and some as recently as latest Pleistocene (25-10 ka).

Our morphometric data suggest that significant surface rupturing of early(?) Holocene or latest Pleistocene age may have occurred on the Cañon fault (6), which is the southernmost segment of the Sangre de Cristo fault zone, southeast of Taos. The Cedro Canyon fault (3) and the northern segment of the Taos Pueblo fault (5) show clear evidence of latest Pleistocene movement. In addition, the Mesita (1), Sunshine Valley (2), and Urraca Ranch (4) faults, the southern segment of the Taos Pueblo fault (5), and, possibly, the Embudo fault (8) show evidence of most recent movement in late Pleistocene time. Los Cordovas faults (7) are known only to be younger than the Pliocene to lower(?) Pleistocene deposits that they displace;

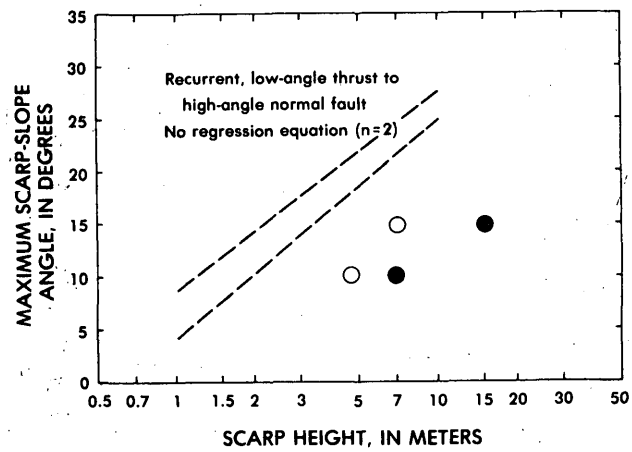

Figure 9.—Maximum scarp-slope angle (θ) plotted against scarp heights (Hs and Hm) for the Embudo fault (fault 8 on the accompanying map). Open circles are for most recent single-event part of scarp; filled circles are for entire multiple-event scarp.

however, we suspect they may have been active in middle Pleistocene time.

Fault scarps formed in middle to upper Pleistocene surficial deposits in the study area are as much as 18 m high; those faults that show recurrent movement generally have scarps more than 7 m high. The highest scarps are in Pliocene to lower Pleistocene deposits along Los Cordovas and the Embudo faults and in lower to middle Pleistocene alluvium along the Cedro Canyon fault; these scarps are clearly the product of recurrent movement as evidenced by decreasing amounts of displacement in progressively younger deposits.

The Sangre de Cristo fault zone and the Embudo fault form the eastern and southeastern boundaries, respectively, of the Pliocene to Pleistocene Rio Grande rift in the Taos Plateau area of northern New Mexico. Farther south, in the Española basin, the Embudo and Pajarito faults form the north and west margins, respectively, of the rift. The Embudo fault coincides with the Jemez lineament, which is marked by a regional alinement of Quaternary volcanic centers. Across this lineament, the rift abruptly changes geometry from the deep, east-dipping basin below the Taos Plateau of the southern San Luis basin to the shallower, west-dipping Española basin.

Many faults on the Taos Plateau have displaced Pliocene and Quaternary deposits. In view of the distribution, size, and number of faults that could have histories of recurrent movement in this area, earthquakes and surface ruptures may have been associated with hundreds of faults or fault segments during the past 5 Ma. Servilleta Basalt along the Sangre de Cristo fault zone near the Colorado-New Mexico state line has been displaced from a minimum of 240-360 m to perhaps as much as 600 m. These data indicate a minimum uplift rate of 60-120 m/m.y. for the past 3-4 Ma, rates that are comparable to those estimated for other major rift-bounding fault zones in central and southern New Mexico.

Table 3.--Scarp morphology data for some faults on the Taos Plateau

[Symbols: *, data not used in regression equation; ---, not determined; n, number of data pairs; r^2, coefficient of determination]

Profile number	Scarp angle, θ (in degrees)	Scarp height (in m) Single (Hs)	Scarp height (in m) Multiple (Hm)	Remarks
Cedro Canyon fault (3), near Costilla, N. Mex.				
m3-1	18.0	4.2	9.6	
m3-2	20.5	6.1	11.1	
m3-3	20.0	5.8	11.9	
m3-4	21.0	6.1	10.6	
m3-5	23.5	7.2	11.0	
m3-6	24.0	7.9	13.8	θ approximate.
m3-7	22.75	6.8	11.1	
m3-8	17.5	5.5*	9.9	Hs approximate.
m3-9	16.25	2.4*	---	Scarp partly buried at toe.
m3-10	10.75	1.2*	3.8	Hs approximate.
m3-11	9.75	1.7	4.2	
m3-12	9.1	1.1*	---	Scarp partly buried at toe.
Regression equations:	θ = 4.7 + 21.1 (log Hs)	n=8	r^2=0.98	
	θ =-4.7 + 24.6 (log Hm)	n=10	r^2=0.88	
Taos Pueblo fault (5), near Taos, N. Mex.				
Southern segment:				
m5-1	10.0	4.3	6.2	
m5-2	12.0	2.8	6.2	
m5-3	11.5	3.6	5.0	
Northern segment:				
m6-1	15.25	3.9	7.0	Lower part of double scarp.
m6-2	20.0	6.8	11.6	Upper part of double scarp.
m6-3	14.1	3.3	4.6	Lower part of double scarp.
m6-4	16.0	4.5	7.3	Upper part of double scarp.
m6-5	15.5	3.7	5.1	
Regression equations:				
Southern segment:	none			
Northern segment:	θ = 4.7 + 18.2 (log Hs)	n=5	r^2=0.96	
	θ = 5.3 + 13.3 (log Hm)	n=5	r^2=0.80	
Cañon fault (6), east of Taos, N. Mex.				
m4-1	15.75	3.4	---	
m4-2	16.25	2.95	---	
m4-3	13.25	1.8	5.4	
m4-4	14.75	2.4	>3.8*	Scarp partly buried.
m4-5	10.5	1.75	3.5	
m4-6	10.75	1.9	4.5	
m4-7	10.0	---	4.1	
Regression equations:	θ = 7.0 + 18.0 (log Hs)	n=6	r^2=0.71	
	θ = 1.5 + 15.2 (log Hm)	n=4	r^2=0.52	
Embudo fault (8), near Arroyo Hondo, N. Mex.				
m7-1	15.0	7.1	15.2	
m7-2	10.4	4.7(?)	>7.0	Crest eroded, Hm minimum.
Regression equation:	none			

REFERENCES CITED

Aldrich, M. J., and Laughlin, A. W., 1982, Orientation of least-principal horizontal stress—Arizona, New Mexico, and the Trans-Pecos area of West Texas: Los Alamos National Laboratory Publication LA-9158-Map UC-11, scale 1:1,000,000.

Baldridge, W. S., Bartov, Y., and Kron, A., 1983, Geologic map of the Rio Grande rift and southeastern Colorado Plateau, New Mexico and Arizona, in Riecker, R. E., ed., Rio Grande rift—Tectonics and magmatism: Washington, D.C., American Geophysical Union, scale 1:500,000.

Baldridge, W. S., Damon, P. E., Shafiqullah, M., and Bridwell, R. J., 1980, Evolution of the central Rio Grande rift, New Mexico—new potassium-argon ages: Earth and Planetary Science Letters, v. 51, p. 309-321.

Bucknam, R. C., and Anderson, R. E., 1979, Estimation of fault-scarp ages from a scarp-height-slope-angle relationship: Geology, v. 7, no. 1, p. 11-14.

Budding, A. J., 1978, Subsurface geology of the Pajarito Plateau—interpretation of gravity data, in Hawley, J. W., compiler, Guidebook to the Rio Grande rift in New Mexico and Colorado: New Mexico Bureau of Mines and Mineral Resources Circular 163, p. 196-198.

Burroughs, R. L., 1978, Northern rift guide 2—Alamosa to Antonito, Colorado, in Hawley, J. W., compiler, Guidebook to the Rio Grande rift in New Mexico and Colorado: New Mexico Bureau of Mines and Mineral Resources Circular 163, p. 33-36.

Chapin, C. E., 1979, Evolution of the Rio Grande rift—a summary, in Riecker, R. E., ed., Rio Grande rift—Tectonics and magmatism: Washington, D.C., American Geophysical Union, p. 1-5.

Chapin, C. E., and Seager, W. R., 1975, Evolution of the Rio Grande rift in the Soccoro and Las Cruces areas, in Seager, W. R., Clemons, R. E., and Callender, J. F., eds., Guidebook to Las Cruces country: New Mexico Geological Society, 26th Field Conference, 1975, p. 297-321.

Colton, R. B., 1976, Map showing landslide deposits and late Tertiary and Quaternary faulting in the Fort Garland-San Luis area, Colorado-New Mexico: U.S. Geological Survey Open-File Report 76-185.

Cordell, Lindreth, 1978, Regional geophysical setting of the Rio Grande rift: Geological Society of America Bulletin, v. 89, p. 1073-1090.

Galusha, Ted, and Blick, J. C., 1971, Stratigraphy of the Santa Fe Group, New Mexico: American Museum of Natural History Bulletin 144, 127 p.

Golombek, M. T., 1983, Geology, structure and tectonics of the Pajarito fault zone in the Española basin of the Rio Grande rift, New Mexico: Geological Society of America Bulletin, v. 94, p. 192-205.

Hawley, J. W., compiler, 1978, Guidebook to the Rio Grande rift in New Mexico and Colorado: New Mexico Bureau of Mines and Mineral Resources Circular 163, 241 p.

Hawley, J. W., Bachman, G. O., and Manley, Kim, 1976, Quaternary stratigraphy in the Basin and Range, Southern Rocky Mountains, and Great Plains Provinces, New Mexico and western Texas, in Mahaney, W. C., ed., Quaternary stratigraphy of North America: Stroudsburg, Pa., Dowden, Hutchinson, and Ross, p. 235-274.

Kelley, V. C., 1977, Geology of the Española Basin, New Mexico: New Mexico Bureau of Mines and Mineral Resources Geologic Map 48, scale 1:125,000.

Kirkham, R. M., and Rodgers, W. P., 1981, Earthquake potential in Colorado—a preliminary evaluation: Colorado Geological Survey Bulletin 43, 171 p.

Lambert, P. W., 1966, Notes on the late Cenozoic geology of the Taos-Questa area, New Mexico, in Northrop, S. A., and Read, C. B, eds.; Guidebook of Taos-Raton-Spanish Peaks country, New Mexico and Colorado: New Mexico Geological Society, 17th Field Conference, 1966, p. 43-50.

Lipman, P. W., 1981, Volcano-tectonic setting of Tertiary ore deposits, southern Rocky Mountains, in Dickinson, W. R., and Payne, W. D., eds., Relations of tectonics to ore deposits in the southern cordillera: Arizona Geological Society Digest, v. 14, p. 199-213.

——1983, Cenozoic magmatism associated with extensional tectonics in the Rocky Mountains [abs.]: Geological Society of America Abstracts with Programs, v. 15, no. 5, p. 288.

Lipman, P. W., and Mehnert, H. H., 1975, Late Cenozoic basaltic volcanism and development of the Rio Grande depression in the Southern Rocky Mountains, in Curtis, Bruce, ed., Cenozoic history of the Southern Rocky Mountains: Geological Society of America Memoir 144, p. 119-154.

——1979, The Taos Plateau volcanic field, northern Rio Grande rift, New Mexico, in Riecker, R. E., ed., Rio Grande rift—Tectonics and magmatism: Washington, D.C., American Geophysical Union, p. 289-312.

Lipman, P. W., Steven, T. A., and Mehnert, H. H., 1970, Volcanic history of the San Juan Mountains, Colorado, as indicated by potassium-argon dating: Geological Society of America Bulletin, v. 81, no. 8, p. 2329-2352.

Luedke, R. G., and Smith, R. L., 1978, Map showing distribution, composition, and age of late Cenozoic volcanic centers in Arizona and New Mexico: U.S. Geological Survey Miscellaneous Investigations Series I-1091-A, 2 sheets, scale 1:1,000,000.

Machette, M. N., 1980, Seismotectonic analysis of the Rio Grande rift, New Mexico, in Evernden, J. F., ed., Summaries of technical reports, Volume IX—National Earthquake Hazards Reduction Program: U.S. Geological Survey Open-File Report 80-6, p. 56-57.

Machette, M. N., and Colman, S. M., 1983, Age and distribution of Quaternary faults in the Rio Grande rift—Evidence from morphometric analysis of fault scarps [abs.]: Geological Society of America Abstracts with Programs, v. 15, no. 5, p. 320.

Machette, M. N., and McGimsey, R. G., 1983, Map of Quaternary and Pliocene faults in the Socorro and western part of the Fort Sumner 1° x 2° quadrangles, central New Mexico: U.S. Geological Survey Miscellaneous Field Studies Map MF-1465-A with pamphlet, scale 1:250,000.

Manley, Kim, 1976, K-Ar age determinations on Pliocene basalts from the Española basin, New Mexico: Isochron/West, no. 16, p. 29-30.

_____1978, Structure and stratigraphy of the Española basin, New Mexico: U.S. Geological Survey Open-File Report 78-667, 24 p.

_____1979, Structure and stratigraphy of the Española basin, Rio Grande rift, in Riecker, R. E., ed., Rio Grande rift—Tectonics and magmatism: Washington D.C., American Geophysical Union, p. 71-86.

Manley, Kim, and Mehnert, H. H., 1981, New K-Ar ages for Miocene and Pliocene volcanic rocks in the northwestern Española basin and their relationships to the history of the Rio Grande rift: Isochron/West, no. 30, p. 5-8.

Manley, Kim, Scott, G. R., and Wobus, Reinhard, compilers, 1978, Preliminary geologic map of the Aztec 1° x 2° quadrangle, northwestern New Mexico and southwestern Colorado: U.S. Geological Survey Open-File Report 78-466, scale 1:250,000.

McCalpin, James, 1983, Quaternary geology and neotectonics of the west flank of the northern Sangre de Cristo Mountains, south-central Colorado: Colorado School of Mines Quarterly, v. 77, no. 3, 97 p.

McKinlay, P. F., 1956, Geology of Costilla and Latir Peak quadrangles, Taos County, New Mexico: New Mexico Bureau of Mines and Mineral Resources Bulletin 42, 32 p.

Miller, J. P., Montgomery, Arthur, and Sutherland, P. K., 1963, Geology of part of the southern Sangre de Cristo Mountains, New Mexico: New Mexico Bureau of Mines and Mineral Resources Memoir 11, 106 p.

Muehlberger, W. R., 1979, The Embudo fault between Pilar and Arroyo Hondo, New Mexico—An active intracontinental transform fault, in Ingersoll, R. A., ed., Guidebook to Santa Fe country: New Mexico Geological Society, 30th Field Conference, 1979, p. 77-82.

Muehlberger, W. R., Peterson, C. M., and Leinberger, R. L., 1983, Late Cenozoic stratigraphy and structure of the Taos Plateau, Rio Grande graben, New Mexico [abs]: Geological Society of America Abstracts with Programs, v. 15, no. 5, p. 321.

Nash, D. B., 1981, FAULT: A Fortran program for modelling the degradation of active normal fault scarps: Computers and Geosciences, v. 7, p. 249-266.

Ozima, M., Kono, M., Kaneoka, I., Kinoshita, H., Kobayashi, Kazuo, Nagata, Takesi, Larson, E. E., and Strangway, D. W., 1967, Paleomagnetism and potassium-argon ages of some volcanic rocks from the Rio Grande gorge, New Mexico: Journal of Geophysical Research, v. 72, no. 10, p. 2615-2621.

Pierce, K. L., 1981, Quaternary dating and neotectonics, in Charonnat, B. B., and others, compilers, Summaries of technical reports, Volume XII—National Earthquake Hazards Reduction Program: U.S. Geological Survey Open-File Report 81-833, p. 154-156.

Scott, G. R., 1970, Quaternary faulting and potential earthquakes in east-central Colorado: U.S. Geological Survey Professional Paper 700-C, p. C11-C18.

Scott, W. R., McCoy, W. D., Shroba, R. R., and Rubin, Meyer, 1983, Reinterpretation of the exposed record of the last two cycles of Lake Bonneville, Western United States: Quaternary Research, v. 20. no. 3, p. 261-285.

Seager, W. R., 1981, Geology of the Organ Mountains and southern San Andres Mountains, New Mexico: New Mexico Bureau of Mines and Mineral Resources Memoir 36, 97 p.

Strain, W. S., 1966, Blancan mammalian fauna and Pleistocene formations, Hudspeth County, Texas: University of Texas at Austin, Texas Memorial Museum Bulletin 10, 55 p.

Tweto, Ogden, 1979, Geologic map of Colorado: Reston, Va., U.S. Geological Survey, scale 1:500,000.

Upson, J. E., 1939, Physiographic subdivisions of the San Luis Valley, southern Colorado: Journal of Geology, v. 47, p. 721-736.

Wallace, R. E., 1977, Profiles and ages of young fault scarps, north-central Nevada: Geological Society of America Bulletin, v. 88, no. 9, p. 1267-1281.

Woodward, L. A., Callender, J. F., and Zilinski, R. E., 1975, Tectonic map of the Rio Grande rift, New Mexico: Geological Society of America Map and Chart Series MC-11, scale 1:500,000.

Zoback, M. L., Anderson, R. E., and Thompson, G. A., 1981, Cainozoic evolution of the state of stress and style of tectonism of the Basin and Range Province of the Western United States: Philosophical Transactions of the Royal Society of London, series A, v. 300, p. 407-434.

Zoback, M. L., and Zoback, Mark, 1980, State of stress in the conterminous United States: Journal of Geophysical Research, v. 85, B11, p. 6113-6156.